INSTITUTE OF PHYSICS PUBLISHING SUPERCONDUCTOR SCIENCE AND TECHNOLOGY

Supercond. Sci. Technol. **18** (2005) S297–S302 doi:10.1088/0953-2048/18/12/012

# Relationship between the $n$-value and critical current in $Nb_3Sn$ superconducting wires exhibiting intrinsic and extrinsic behaviour

**David M J Taylor and Damian P Hampshire**

Superconductivity Group, Physics Department, Durham University, Durham DH1 3LE, UK
and
Grenoble High Magnetic Field Laboratory, BP 166, 38042 Grenoble Cedex 9, France

E-mail: d.p.hampshire@dur.ac.uk

Received 5 August 2005, in final form 3 October 2005
Published 4 November 2005
Online at stacks.iop.org/SUST/18/S297

**Abstract**

The relationship between the $n$-value and critical current ($I_C$) is investigated for six different ITER-candidate $Nb_3Sn$ wires characterized as a function of magnetic field ($B \leqslant 28$ T), temperature (4.2 K $\leqslant T \leqslant$ 12 K) and intrinsic axial strain ($-1\% \leqslant \varepsilon_I \leqslant +0.4\%$). For the five wires exhibiting intrinsic behaviour, $n(I_C)$ can be parameterized by a modified power law of the form $n = 1 + rI_C^s$, where $s$ is a constant with a value of $0.41 \pm 0.03$. The parameter $r$ decreases as the magnitude of the intrinsic strain increases and is a relatively weak function of temperature. For one of the wires, the $n$-value saturates at high critical currents (low magnetic fields), characteristic of extrinsic filament nonuniformities.

(Some figures in this article are in colour only in the electronic version)

## 1. Introduction

The $n$-value is commonly used to characterize the sharpness of the electric field–current density ($E$–$J$) transition in technological superconductors [1–6]. Together with the critical current density ($J_C$), the $n$-value is important in applications such as persistent-mode NMR magnets [7] for extrapolating to the low operating electric fields, and cable-in-conduit-conductor fusion magnets for calculating operating margins and interpreting data for prototype systems [8–10]. The origin of the $n$-value in low-temperature superconducting wires is generally attributed to distributions in the critical current [5, 6, 11–18] arising from distributions in the elementary flux-pinning forces (intrinsic effects) [6, 11–14] and from nonuniformities in the cross-sectional area of the superconducting filaments (extrinsic effects) [5, 16–18]. Both intrinsic and extrinsic factors will generally affect the $n$-value, although the correlations between filament nonuniformities and low $n$-values observed in some Nb–Ti wires [5, 18] have lead to the $n$-value being commonly used as a 'quality index' [4]. The critical current density and $n$-value in $Nb_3Sn$ superconducting wires vary strongly as a function of magnetic field ($B$), temperature ($T$) and intrinsic axial strain ($\varepsilon_I$), which must be accurately described for the purposes of magnet design. Considerable research effort has been directed at developing scaling laws for parameterizing $J_C(B, T, \varepsilon_I)$ data [19–25], but there is currently no accepted framework for describing the variation of the $n$-value with field, temperature and strain. One possible approach is to relate the $n$-value to the critical current density. Experimental data presented as plots of $n$ versus $J_C$ show strong correlations, and various formulae have been proposed [8, 9, 26], while the existence of such a relationship is also suggested by some theoretical models [11, 15]. In this paper, we investigate the relationship between the $n$-value and critical current density for a number of $Nb_3Sn$ superconducting wires characterized as a function of field, temperature and strain, and seek to develop a mathematical description of the $n$-value covering the full range of parameter space.

## 2. Experimental techniques

Voltage–current ($V$–$I$) measurements were performed on six different types of ITER-candidate $Nb_3Sn$ wire over various

**Table 1.** The experimental range (temperature, magnetic field and intrinsic strain) over which the six different wires were investigated.

| | Experimental range | | |
|---|---|---|---|
| Wire | Temperature (K) | Field (T) | Intrinsic strain (%) |
| OST | 4.2–12 | ⩽28 | −1.11 to +0.15 |
| OKSC | 4.2–14 | ⩽28 | −1.11 to +0.18 |
| EM-LMI | 4.2–12 | ⩽23 | −0.76 to +0.21 |
| Fur | 4.2 | ⩽15 | −1.29 to +0.41 |
| Vac(A) | 4.2–12 | ⩽23 | −1.07 to +0.39 |
| Vac(B) | 4.2 | ⩽23 | −0.98 to +0.17 |

ranges of magnetic field, temperature and intrinsic strain (see table 1). A similar experimental procedure was employed for all of the wires investigated. Standard heat treatments [27–29] were performed under argon with the wires mounted on oxidized stainless-steel mandrels. The reacted wires were then etched in hydrochloric acid to remove the chrome plating, transferred to helical (Walters) springs and attached by copper plating and soldering. Measurements were performed using the Durham strain probe [29, 30], enabling strains to be applied to the wire via the rotation of one end of the spring. The wires were immersed in a liquid helium bath at 4.2 K or located in a variable-temperature enclosure with three independently controlled Cernox thermometers and constantan wire heaters. Experiments were carried out in fields up to 23 or 28 T using resistive magnets at the European high-field laboratory in Grenoble, or in fields up to 15 T using a superconducting magnet in Durham. At particular values of field, temperature and strain, the current in the wire was slowly increased and the voltage across a section of the wire (typical tap separation: 20 mm) was measured using a nanovolt amplifier and digital voltmeter. The electric field ($E$) and engineering current density ($J$) were calculated from $V$ and $I$ by dividing by the tap separation and the total cross-sectional area of the wire respectively (all of the wires are 0.81 mm in diameter). Critical currents and $n$-values were calculated after the current in the normal shunt (typically 50 mA at 10 $\mu$V m$^{-1}$, measured above the critical temperature) had been subtracted from the total current. Various spring geometries and materials were used for the different wires, but it has been shown that the superconducting properties are generally universal functions of intrinsic axial strain calculated at the midpoint of the wire, independent of the type of spring [29]. In all of the measurements, tensile strains and then compressive strains were applied to the wires. For three wires (OST, OKSC and EM-LMI), measurements at 4.2 K and at variable temperature were performed on the same sample on two separate strain cycles. In all cases, tests show that the critical currents are reversible to within ∼4% after the various cycles. For two wires (EM-LMI and Vac(A)), measurements were performed on different samples in Durham (up to 15 T) and in Grenoble (up to 23 T), and the critical current data were found to agree to within ∼2%.

## 3. Results

Figure 1(a) shows a typical set of $E$–$J$ characteristics at different values of intrinsic strain (defined as the strain relative to the peak in $J_C$ [29, 31–33]). A power-law relationship

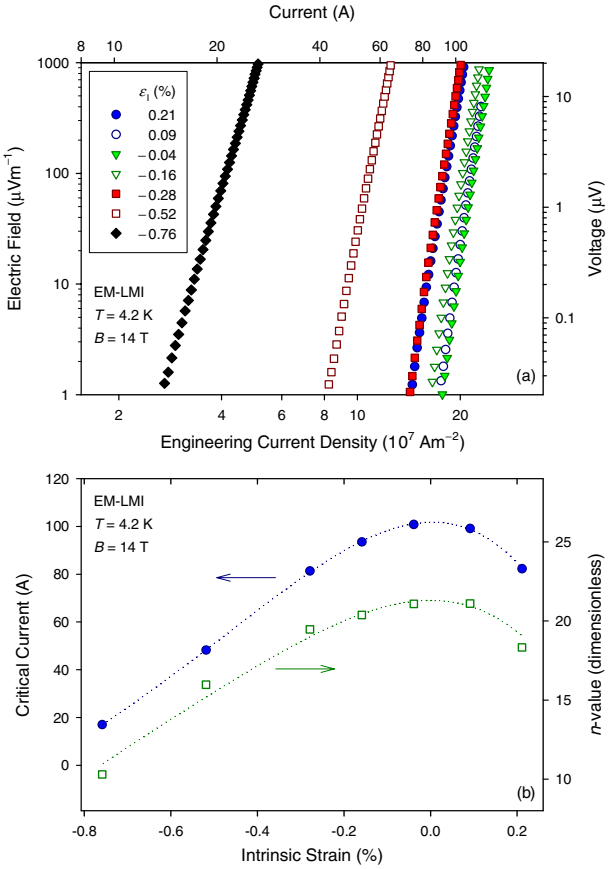


**Figure 1.** (a) Log–log plot of electric field versus engineering current density (voltage versus current) for the EM-LMI wire at different intrinsic strains at 4.2 K and 14 T. (b) The critical current and $n$-value of the EM-LMI wire as a function of intrinsic strain at 4.2 K and 14 T. The critical current is defined at 10 $\mu$V m$^{-1}$ and the $n$-value calculated between 10 and 100 $\mu$V m$^{-1}$. The symbols show the measured data; the dotted curves are guides to the eye.

between $E$ and $J$ is observed, and the $n$-value can be defined via the following relationship [2]:

$$E(J, B, T, \varepsilon_I) = E_C[J/J_C(B, T, \varepsilon_I)]^n. \quad (1)$$

Figure 1(b) shows the critical currents ($I_C$) and $n$-values obtained from the $E$–$J$ characteristics in figure 1(a), where, as is standard, the critical current is defined at an electric-field criterion of 10 $\mu$V m$^{-1}$ and the $n$-value is calculated between 10 and 100 $\mu$V m$^{-1}$. These standard criteria are used for the most of the critical current and $n$-value data presented in this paper (except the low $E$-field data in figure 8). It can be seen in figure 1(b) that the critical current and $n$-value have a similar inverted parabolic behaviour as a function of intrinsic strain, motivating the analysis of the relationship between $n$ and $I_C$ that follows. The scatter in the $n$-value data (e.g. figure 1(b)) can be attributed to systematic variations in the temperature of the wire during the $E$–$J$ transition (from 10 to 100 $\mu$V m$^{-1}$). Assuming a maximum variation of 20 mK [29], the associated errors in the $n$-value are estimated at typically 4%.

Figures 2–4 show the $n$-value plotted as a function of critical current for the six different wires investigated. In all of the figures, each set of points represents variable-field

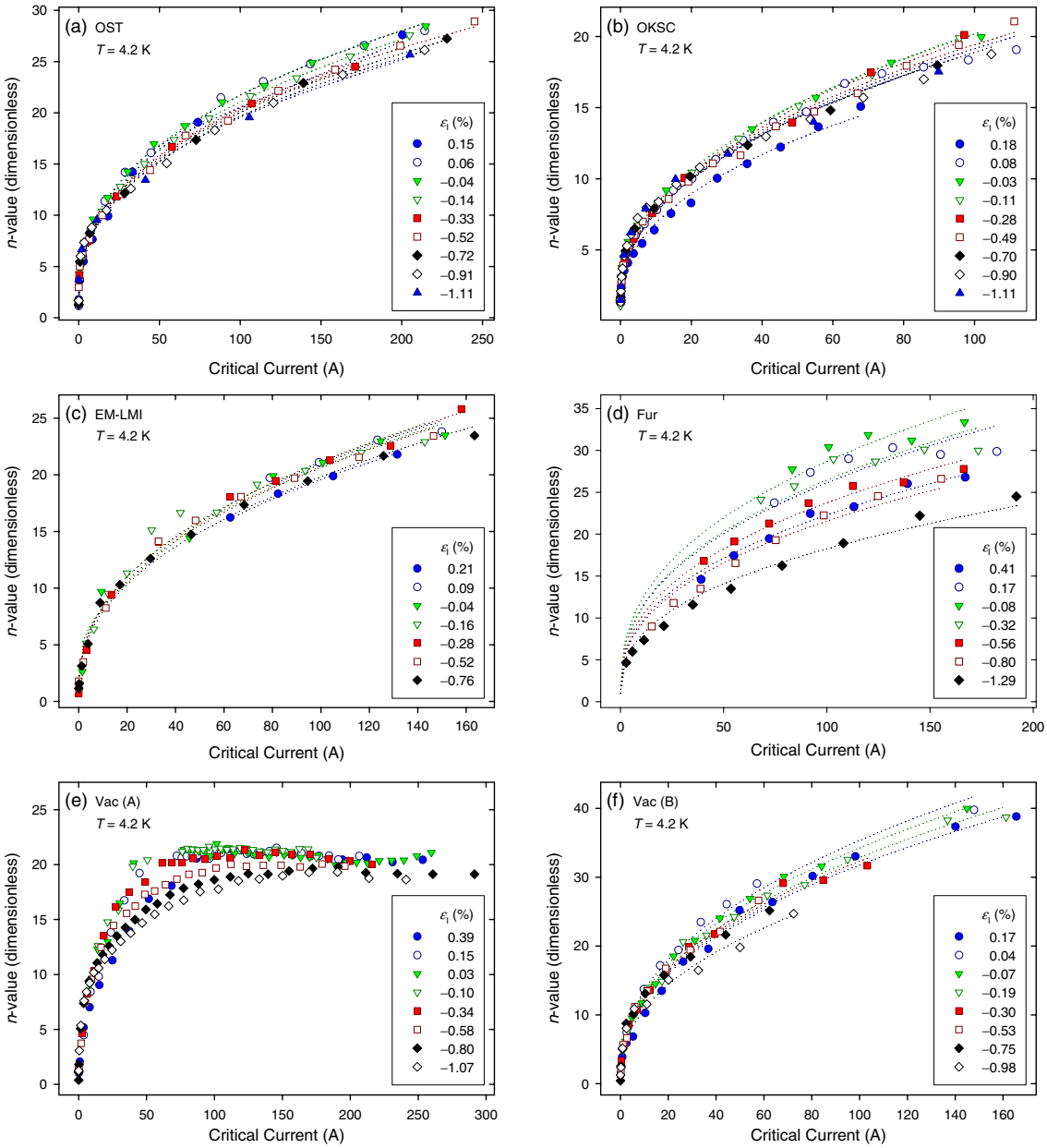


**Figure 2.** The $n$-value as a function of critical current for a number of $Nb_3Sn$ wires at a temperature of 4.2 K and at different intrinsic strains. The symbols show the measured data; the dotted curves show the fits made using equation (2) with a single value of $s$ for each wire.

data at constant temperature and strain. Figures 2 and 3 show datasets at different intrinsic strains at 4.2 and 12 K respectively. Figure 4 shows datasets at different temperatures at constant intrinsic strain. It can be seen that, for all of the wires except Vac(A), there is a similar form for $n$ versus $I_C$ at a particular temperature and strain. The $n$-values are not universal functions of critical current, but $n$ at constant $I_C$ is a relatively weak function of intrinsic strain and temperature. For example, $n$ at constant $I_C$ varies by typically 10–20% as a function of intrinsic strain at 4.2 K, with the exception of the Furukawa wire, which shows a considerably stronger variation (see figure 2(d)).

For the Vac(A) wire, the $n$-value tends to a saturation value at high critical currents (low magnetic fields). This saturation behaviour was reported previously: the saturation value of $n$ decreases with increasing $|\varepsilon_I|$ and with decreasing electric-field criterion [2]. Figure 5 compares $I_C$ and $n$-value data for the Vac(A) and Vac(B) wires: the values of critical current are similar, but the $n$-values differ considerably at low magnetic fields. The two wires come from different billets that were nominally identical prior to extrusion, and it is believed that the extrusion process for one of the billets (Vac(A)) caused the reduced $n$-values at low fields [34]. The behaviour of the Vac(A) wire is characteristic of extrinsic 'sausaging' effects and is discussed in section 5.

## 4. Analysis

A power-law relationship between $n$-value and critical current has been used previously [8, 26]. For all of the wires

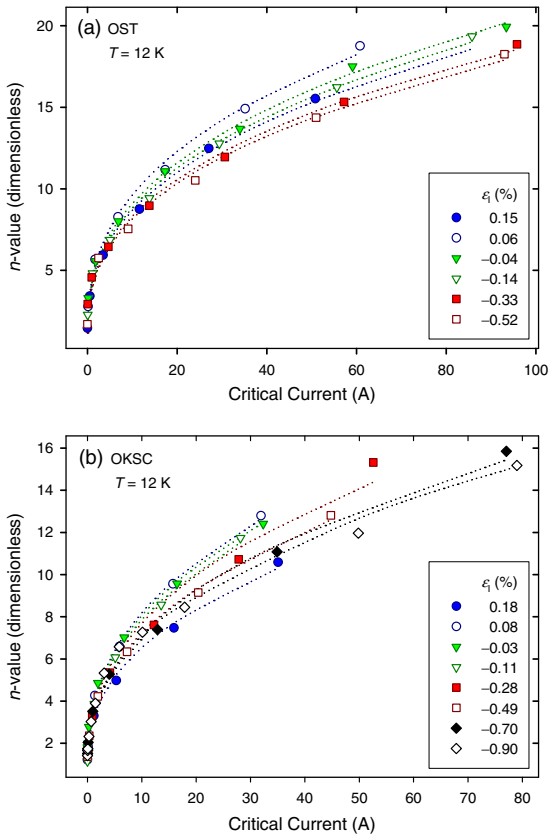


**Figure 3.** The $n$-value as a function of critical current for the OST and OKSC $Nb_3Sn$ wires at a temperature of 12 K and at different intrinsic strains. The symbols show the measured data; the dotted curves show the fits made using equation (2) with a single value of $s$ for each wire.

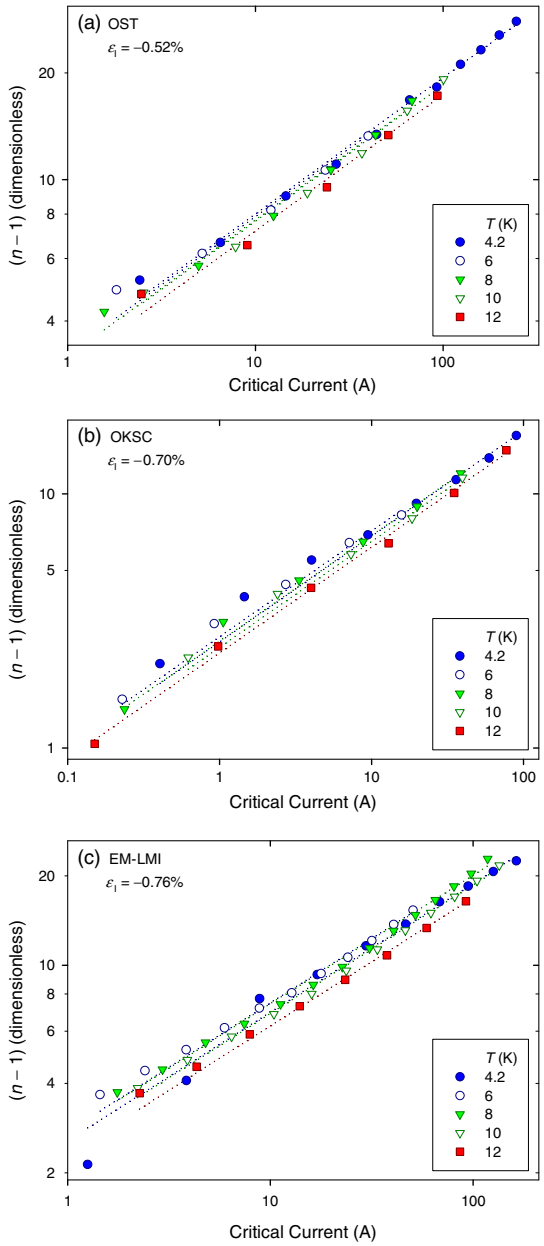


**Figure 4.** A log–log plot of $(n-1)$ versus critical current for a number of $Nb_3Sn$ wires at constant values of intrinsic strain and at different temperatures between 4.2 and 12 K. The symbols show the measured data; the dotted lines show the fits made using equation (2) with a single value of $s$ for each wire.

investigated, we find that $n \to \sim 1$ as $I_C \to 0$, and hence a better fit to the data can be obtained using the modified power law:

$$n(B, T, \varepsilon_I) = 1 + r(T, \varepsilon_I)[I_C(B, T, \varepsilon_I)]^{s(T,\varepsilon_I)}. \qquad (2)$$

Equation (2) was used to fit the $n$-value data for five of the wires investigated, as shown in figures 2–6 (accurate fits to the $n$-value data for the Vac(A) wire were not possible). The curvature at low values of $n(I_C)$ in the standard log–log plot (figure 6 inset) explicitly shows that the data are fitted less accurately using a standard power-law relationship [8, 26]. The fitting parameters $r$ and $s$ are, in principle, functions of temperature and strain. However, it is found that variations in the optimum values of the exponent $s(T, \varepsilon_I)$ are relatively small ($\pm 15\%$) and nonsystematic, while reasonably accurate parameterizations can be achieved by using a constant value of $s$ for a particular wire. The optimum values of $s$ are similar for all of the wires and are in the range 0.38–0.44 (see figure 7(a)).

With $s$ = constant, the parameter $r(T, \varepsilon_I)$ then determines the temperature and strain dependences of $n$ at constant $I_C$. Figure 7(a) shows how $r$ varies with intrinsic strain at 4.2 K (cf figure 2). Despite the scatter on the data, it can be seen that, for all of the wires, $r$ is a maximum at approximately zero intrinsic strain and decreases with increasing tensile or compressive intrinsic strains. For the Furukawa wire, $r$ varies by $\sim 40\%$ over the investigated strain range, while for the other four wires the variations are between $\sim 10\%$ and $\sim 20\%$. Figure 7(b) shows how $r$ varies with temperature at constant values of intrinsic strain for three of the wires investigated (cf figure 4). Similar temperature dependences for $r$ are observed at all values of intrinsic strain (graphs not shown). It can be seen that $r$ varies by $\sim 10\%$ in the temperature range 4.2–12 K. For all of the wires, $r$ decreases monotonically with increasing temperature between 6 and 12 K, but for the OKSC and EM-LMI wires, $r$ is lower at 4.2 K than at 6 K, perhaps due to differences in the temperature stability (see section 3) or the different strain cycles on which the data were obtained.

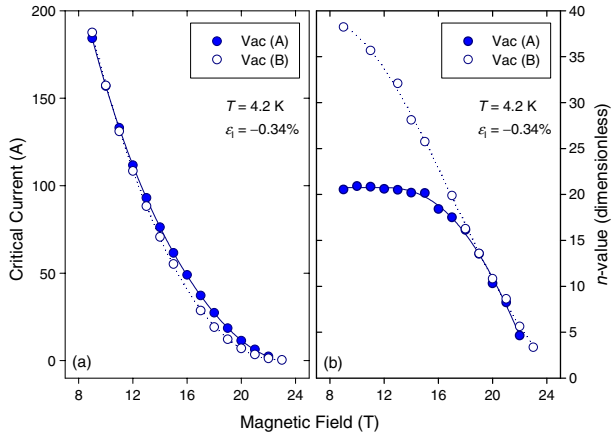


**Figure 5.** (a) The critical current and (b) the $n$-value of the Vac wires from two different billets as a function of magnetic field at 4.2 K and −0.34% intrinsic strain.

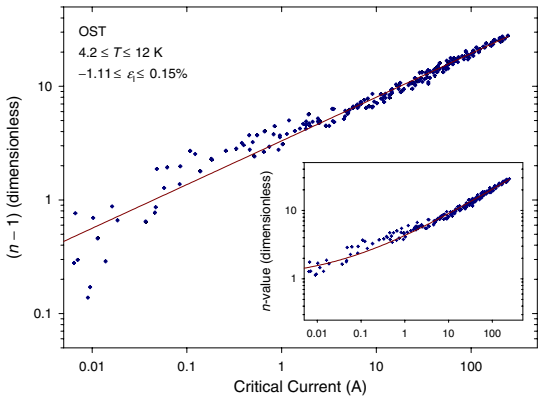


**Figure 6.** A log–log plot of $(n-1)$ versus critical current for the OST wire (data are shown at all values of field, temperature and strain investigated). Inset: log–log plot of $n$-value versus critical current. The symbols show the measured data; the line and curve show a universal fit made using equation (2).

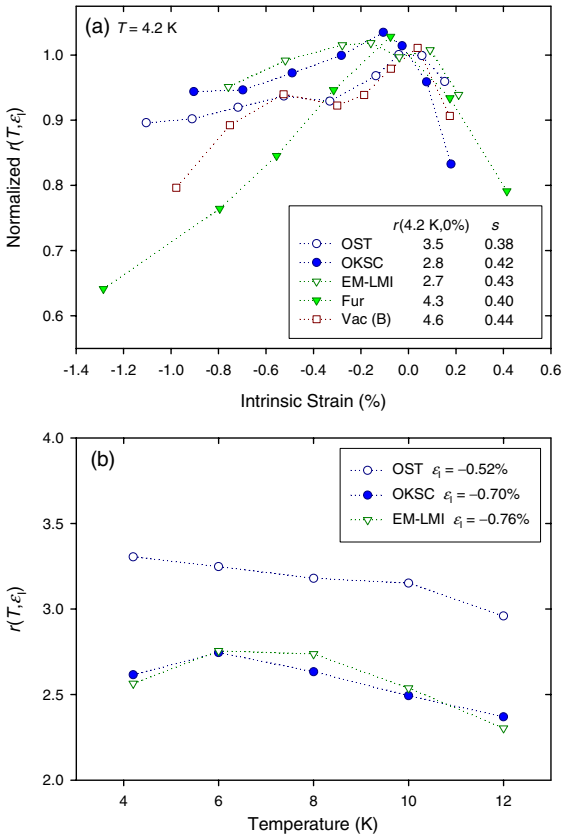


**Figure 7.** (a) The parameter $r(T, \varepsilon_I)$ (normalized to its value at $\varepsilon_I = 0$) as a function of intrinsic strain at 4.2 K for five $Nb_3Sn$ wires. The legend shows the values of $r(T = 4.2\ \mathrm{K}, \varepsilon_I = 0)$ and the values of the exponent $s$ for each wire. (b) The parameter $r$ as a function of temperature at constant values of intrinsic strain (see legend) for three $Nb_3Sn$ wires.

Figure 8 compares $n$ versus $I_C$ plots calculated at lower electric-field criteria (1 $\mu$V m$^{-1}$ for $I_C$ and 1–10 $\mu$V m$^{-1}$ for $n$) with plots calculated at the standard criteria (10 and 10–100 $\mu$V m$^{-1}$). All of the datasets can be parameterized using equation (2) and it is found that the optimum values for the exponent $s$ are similar (to within 0.02) for the datasets obtained at the different $E$-field criteria. The values of $r$ are considerably higher for the lower electric field data, because $I_C$ decreases with decreasing $E$-field criterion but $n$ increases.

## 5. Discussion and conclusions

Early work on extrinsic Nb–Ti wires considered sausaged filaments with uniform pinning within the filaments [16, 18]. In this case, the distribution of $I_C$ along the length of the filament is entirely due to the distribution in the cross-sectional area (CSA). Hence the $n$-value can be related to the standard deviation of the cross-sectional area $\sigma$(CSA) and the average cross-sectional area $\overline{\mathrm{CSA}}$ by the following expression [11]:

$$n = \left(\frac{\pi}{2}\right)^{1/2}\left(\frac{\overline{\mathrm{CSA}}}{\sigma(\mathrm{CSA})}\right). \qquad (3)$$

Given the uncertainties in the wavelength over which $I_C$ should be averaged, equation (3) is qualitatively in agreement with the results of Ekin [18], who observed a field-independent $n$-value of ∼35 (for 3 T $\leqslant B \leqslant$ 7 T) in a Nb–Ti wire with $\sigma$(CSA) ≈ 5% measured using complementary microscopy. The Vac(A) wire exhibits a similar saturation in the $n$-value, characteristic of extrinsic filament nonuniformities. The saturation value of ∼20 suggests that the effective standard deviation of the sausaging is ∼6% (from equation (3)). The Vac(B) wire, nominally identical prior to extrusion, has similar values of critical current but considerably higher $n$-values in low fields (see figure 5), demonstrating that the $n$-value can be sensitive to factors that do not necessarily affect the critical current [5].

For the five wires exhibiting intrinsic behaviour, the relationship between the $n$-value and critical current can be parameterized by a modified power law with two free parameters $r$ and $s$. We find that $n(B, T, \varepsilon_I)$ cannot be expressed as a universal function of $J_C(B, T, \varepsilon_I)$. The parameter $r(T, \varepsilon_I)$, and hence the $n$-value at constant critical current, varies with both strain and temperature: it generally decreases with increasing $|\varepsilon_I|$, with variations of between ∼10% and ∼40% for the different wires, and has a relatively weak (∼10%) temperature dependence. The origin of these different variations, particularly the strain dependence, remains to be identified. Nevertheless the nearly universal

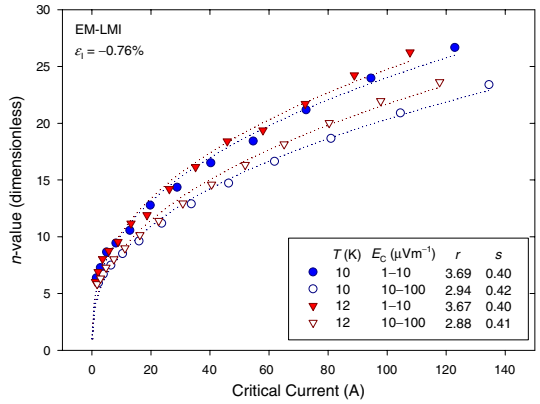


**Figure 8.** The $n$-value as a function of critical current for the EM-LMI $Nb_3Sn$ wire at 10 and 12 K at −0.76% intrinsic strain. The closed symbols are for $I_C$ at 1 $\mu$V m$^{-1}$ and $n$-values between 1 and 10 $\mu$V m$^{-1}$; the open symbols are for $I_C$ at 10 $\mu$V m$^{-1}$ and $n$-values between 10 and 100 $\mu$V m$^{-1}$ (the standard criteria). The dotted curves show the fits made using equation (2) (the legend shows the values of $r$ and $s$).

value of ∼0.41 observed for the exponent $s$ (which is only weakly dependent on the electric-field criterion) will facilitate the parameterization of the $n$-value in $Nb_3Sn$ wires that is required for optimizing magnet design.

## Acknowledgments

The authors acknowledge the support of Ettore Salpietro and Alex Vostner at the European Fusion Development Agency (EFDA), the UK Engineering and Physical Sciences Research Council (EPSRC) and Kozo Osamura through the activities of the Japanese NEDO Grant project (Applied Superconductivity, 2004EA004).

## References

[1] Volker F 1970 *Particle Accelerators* **1** 205
[2] Taylor D M J, Keys S A and Hampshire D P 2002 *Physica* C **372** 1291–4
[3] Bruzzone P 2004 *Physica* C **401** 7–14
[4] Ghosh A K 2004 *Physica* C **401** 15–21
[5] Warnes W H and Larbalestier D C 1986 *Cryogenics* **26** 643–53
[6] Hampshire D P and Jones H 1985 *Magn. Technol.* **9** 531–5
[7] Miyazaki T *et al* 1999 *IEEE Trans. Appl. Supercond.* **9** 2505–8
[8] Mitchell N 2004 *Physica* C **401** 28–39
[9] Martovetsky M 2004 *Physica* C **401** 22–7
[10] Mitchell N 2003 *Fusion Eng. Des.* **66–68** 971–93
[11] Hampshire D P and Jones H 1987 *Cryogenics* **27** 608–16
[12] Baixeras J and Fournet G 1967 *J. Phys. Chem. Solids* **28** 1541–7
[13] Evetts J E and Plummer C J G 1985 *Int. Symp. on Flux Pinning and Electromagnetic Properties of Superconductors (Fukuoka, 1985)* ed T Matsushita, K Yamafuji and F Irie (Fukuoka: Matsukuma) pp 146–51
[14] Wördenweber R 1998 *Rep. Prog. Phys.* **62** 187–236
[15] Edelman H S and Larbalestier D C 1993 *J. Appl. Phys.* **74** 3312–5
[16] Warnes W H 1988 *J. Appl. Phys.* **63** 1651–62
[17] Warnes W H and Larbalestier D C 1986 *Appl. Phys. Lett.* **48** 1403–5
[18] Ekin J W 1987 *Cryogenics* **27** 603–7
[19] Kramer E J 1973 *J. Appl. Phys.* **44** 1360–70
[20] Dew-Hughes D 1974 *Phil. Mag.* **30** 293–305
[21] Taylor D M J and Hampshire D P 2005 *Supercond. Sci. Technol.* **18** S241–52
[22] Keys S A and Hampshire D P 2003 *Supercond. Sci. Technol.* **16** 1097–108
[23] Ekin J W 1980 *Cryogenics* **20** 611–24
[24] Summers L T *et al* 1991 *IEEE Trans. Magn.* **27** 2041–4
[25] ten Haken B, Godeke A and ten Kate H H J 1999 *J. Appl. Phys.* **85** 3247–53
[26] Nijhuis A 2002 *University of Twente Report* No. 21/06/02
[27] Hampshire D P *et al* 2001 *University of Durham Report* No. DurSC0601
[28] Taylor D M J and Hampshire D P 2005 *University of Durham Report* No. EFDA-03-1126
[29] Taylor D M J and Hampshire D P 2005 *Supercond. Sci. Technol.* **18** 356–68
[30] Cheggour N and Hampshire D P 2000 *Rev. Sci. Instrum.* **71** 4521–30
[31] Luhman T, Suenaga M and Klamut C J 1978 *Adv. Cryog. Eng.* **24** 325–30
[32] ten Haken B 1994 *PhD Thesis* University of Twente
[33] Rupp G 1977 *IEEE Trans. Appl. Supercond.* **13** 1565–7
[34] Duchateau J L *et al* 2002 *Supercond. Sci. Technol.* **15** R17–29